



Fig. 5 — Polished section showing fine oxide particles along the bond line of a joint produced at 1050°C under vacuum.

Table 2 — Standard Free Enthalpies of Oxide Formation at 1000°C, kcal

Al ₂ O ₃	SiO ₂	MnO	Cr ₂ O ₃	FeO
205	162	140	127	85

grinding marks on fracture surfaces show that a perfect physical contact of the surfaces was not completed under the welding conditions defined by Ker-goat (Ref. 12).

Pressure was then increased so as to overstep, during a few seconds, the flow stress of the 27CD4 steel between 600 and 800°C. This resulted in a macroscopic welding deformation that

did not exceed 2% of the heated length of the specimens.

Possible segregations of S, P, N and Sb were cited in the literature (Ref. 14). We did not verify this hypothesis.

The adopted welding conditions are given in the section entitled "Optimized welding parameters"; they take into consideration the above analysis.

Results and Discussion

Using the above welding procedure, which resulted in a macroscopic welding deformation that did not exceed 2% of the heated length of the specimens, we carried out mechanical tests and metallographic observations of butt joints. Then, the possible variation ranges of welding temperature and specimen roughness were improved with a short parametric study.

Results from Mechanical Tests

After welding, some specimens are machined for tensile, torsion and impact tests — Fig. 3. The results were compared to those obtained with unwelded samples submitted to the same heat treatment.

The tensile test results shown in Table 3 confirm the validity of our assumption and of the proposed solutions: all the test specimens failed away from the weld interface at the point of maximum necking, in a ductile manner with an elongation equal to those of the base metal, and this for an isothermal anneal (1050°C) of a few seconds. The cooling rates were not perfectly reproducible, which explains the scatter of the experimental tensile strength measurements.

The purpose of this study was to use this process for manufacturing transmission shafts. We tried to characterize the behavior of the joints under torsion

Table 3 — Tensile Properties of Specimens Welded in N₂ (H₂ 5%) (a few seconds at 1050°C)

Tensile strength, MPa	Elongation%	Failure location ^(a)
995	26	MB
955	24	MB
940	21	MB
970	19	MB
1000	17	MB
970	23	MB
995	23	MB
1080	17	MB

(a) MB: failure through base material

with a torsion Amsler machine of the Renault Co. The machine was not well adapted to the dimension of the test specimens produced with the dynamic diffusion welding equipment, and, as a result, it was impossible to use the results of many tests, the tested samples having slipped in the clamping tools. Nevertheless, the single available result is promising although not yet confirmed: we measured a torsion torque of 60 mN for the welded specimens compared with 66 mN for the unwelded pieces having the same microstructure as the weld.

Some authors showed that impact tests characterized the quality of the butt joints more accurately than tensile tests.

Because of the inherent limits of the equipment, we had to carry out these tests with unstandardized impact test specimens. The failure energy was compared to that of the unwelded specimens (Table 4), and this for two different microstructures.

For both structures, the failure energy of joints had similar values, but it was lower than those of unwelded samples. Neither the postweld treatment, nor the ductility of the structure seemed to noticeably change the failure energy of the joints as it was observed in the literature.

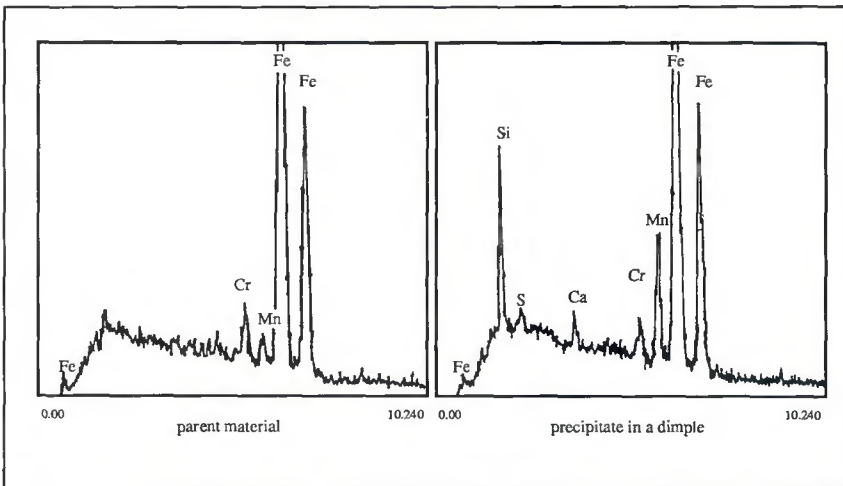


Fig. 6 — EDS analysis spectrum of base material and particles.

Table 4 — Impact Energy of U-Notch Specimens, J

Structure	As-welded	Postweld heat treatment ^(a)
	Bainite	Ferrite and pearlite
Control Specimen	28.2	>50
	27.6	
	28.8	
	28.0	
Welded Specimen	12.8	12.8
	1.4	8.0
	9.0	15.2
	9.4	12.8

(a) 850°C, 15 min, cool to 600°C and hold for 15 min, air cool

